agriculture

MDPI

Article

Predicted Distribution of Locoweed *Oxytropis glabra* in China under Climate Change

Ruijie Huang [1,2], Chenchen Wu [2], Hao Lu [2], Xuemei Wu [1,2] and Baoyu Zhao [2,*]

[1] Department of Animal Husbandry and Fisheries, Guizhou Vocational College of Agriculture, Qingzhen 551400, China; 18786719121@163.com (R.H.); wuxuemei686@163.com (X.W.)
[2] College of Veterinary Medicine, Northwest A&F University, Yangling 712100, China; 2012110050@nwafu.edu.cn (C.W.); luhao@nwafu.edu.cn (H.L.)
* Correspondence: zhaobaoyu12005@nwafu.edu.cn

Abstract: The research on the significant toxic weed *Oxytropis glabra*, which adversely affects the grazing industry and the ecological integrity of natural grasslands in the arid and semi-arid regions of northern China, aims to delineate its potential distribution amidst changing climate conditions. This analysis involves both current conditions (1970–2000) and future projections (2050s and 2070s) under four climate scenarios using an R-optimized MaxEnt model. The results indicate that the distribution of *O. glabra* was primarily influenced by the temperature of the coldest quarter (bio11, ranging from −12.04 to −0.07 °C), precipitation of the coldest quarter (bio19, 0 to 15.17 mm), and precipitation of the warmest quarter (bio18, 0 to 269.50 mm). Currently, the weed predominantly occupies parts of Xinjiang, Inner Mongolia, Gansu, Qinghai, Ningxia, and Tibet. Projections indicate that, across four future climate scenarios, the area of suitable habitats for *O. glabra* is expected to expand and shift toward higher latitudes and elevations. The research provides valuable information and a theoretical foundation for the management of *O. glabra*, alongside advancing grassland ecological research and grazing practices.

Keywords: *Oxytropis glabra*; locoweed; MaxEnt modeling; climate change impacts; toxic plant control; grazing management

Citation: Huang, R.; Wu, C.; Lu, H.; Wu, X.; Zhao, B. Predicted Distribution of Locoweed *Oxytropis glabra* in China under Climate Change. *Agriculture* **2024**, *14*, 850. https://doi.org/10.3390/agriculture14060850

Academic Editor: Abraham J. Escobar-Gutiérrez

Received: 22 April 2024
Revised: 25 May 2024
Accepted: 25 May 2024
Published: 29 May 2024

1. Introduction

Climate significantly influences the geographical distribution of vegetation, and global climate change has profoundly affected the structure and function of grassland ecosystems [1,2]. The Fifth Assessment Report by the Intergovernmental Panel on Climate Change (IPCC) predicts a continued rise in global average temperatures, accompanied by significant changes in precipitation patterns [3]. However, the impact of climate change is not uniform across different regions due to the distinctiveness of natural conditions, leading to varied effects on the growth and distribution of plants [4]. Thus, understanding plant responses to future climate change is crucial for deciphering their survival strategies and for the conservation of biodiversity or the targeted management of invasive species.

Toxic plants are one of the many problems plaguing the development of global grassland livestock farming. Numerous studies have identified locoweed as the most significant toxic plant affecting global grassland pastoralism, primarily due to its toxic alkaloid component, swainsonine [5]. Livestock ingesting locoweed exhibits characteristic symptoms of the disease, potentially resulting in death in severe instances. Locoweed's presence is global, with documented cases of livestock poisoning and consequent economic losses impacting grassland pastoralism in countries such as China, Mongolia, the United States, Brazil, Argentina, and Australia, significantly affecting local pastoral economies [6]. *Oxytropis glabra* DC, a member of the Fabaceae family, is native to China and various regions in Asia and Europe, such as Mongolia, Pakistan, and East European Russia. Conversely, it is considered an introduced species in the United States. In China, this species is recognized as a principal

locoweed. It typically grows in habitats such as mountain grasslands, rocky slopes, saline low-moisture meadows, field ridges, and road edges (Figure 1) [7]. Current research on *O. glabra* primarily investigates its chemical components and activities, toxic effects, treatments for poisoning, endophytes, and feed utilization after detoxification. However, there is a notable scarcity of studies concerning the distribution of suitable habitats for *O. glabra*. Previously, knowledge of these habitats was limited, relying solely on manual field surveys. Moreover, the future impact of climate change on the distribution of suitable habitats for *O. glabra* remains uncertain, impeding effective control measures and pasture management.

Figure 1. *O. glabra* habitat (**A**) and its individual specimens (**B**).

MaxEnt, a Species Distribution Model (SDM) that utilizes the maximum entropy principle, predicts the distribution of species' suitable habitats by employing occurrence points and environmental data [8]. Recognized for its operational simplicity, minimal data requirements, and strong predictive performance, MaxEnt is extensively utilized in conservation efforts for endangered species, invasive species management, pest and disease control, and the cultivation of economic plants [9]. In this study, an R-optimized MaxEnt model and ArcGIS spatial analysis were utilized to investigate the primary environmental variables influencing the distribution of *O. glabra*, the current distribution patterns of its suitable habitats, and potential changes in its distribution under various future climate scenarios. This research fills the research gap by simulating and predicting a suitable habitat for *O. glabra* in China and providing basic information references for the formulation of *O. glabra* prevention and control strategies and pasture management.

2. Materials and Methods

2.1. Species Occurrence Data

Occurrence data for *O. glabra* at the research institute were collected from two primary sources. First, records from field investigations conducted by the corresponding author's research group between 2014 and 2021 were used. These investigations utilized a handheld GPS device (GARMIN GPSMAP 621sc) to capture the latitude and longitude coordinates of *O. glabra* populations in their natural habitats, yielding a total of 441 records. Second, additional data were sourced from online databases, including the Chinese Virtual Herbarium (CVH) and the Global Biodiversity Information Facility (GBIF), with selection criteria focusing solely on records with precise geographic coordinates, resulting in 96 additional records (details are provided in Table S2).

The occurrence data for spatial filtering of *O. glabra* occurrence points were processed using the spThin package in R [10], which removed points within a distance of less than 20 km [11]. The Moran's Index was then calculated using the ArcGIS toolbox to analyze the spatial autocorrelation before and after filtering the occurrence point data [11].

2.2. Environmental Variable Data

The Intergovernmental Panel on Climate Change (IPCC) has developed the Shared Socioeconomic Pathways (SSPs), which consider a variety of factors such as population growth, economic development, technological progress, and resource utilization, building on the foundation of Representative Concentration Pathways (RCPs). SSP126, SSP245, SSP370, and SSP585 represent scenarios titled "Taking the Green Road", "Middle of the Road", "A Rocky Road", and "Taking the Highway", respectively, each with progressively increasing carbon emissions and warming trends [12].

In our initial analysis, we assessed 24 environmental variables, grouped into three main environmental factors crucial for predicting plant distributions: bioclimate, soil, and terrain, as detailed in Table S2 [9]. We sourced data for both current (1970–2000) and future (2050s and 2070s) projections for bioclimate and terrain from the WorldClim database (https://www.worldclim.org/, accessed on 21 January 2022) [13] and soil information from the World Soil Database v1.2 (https://daac.ornl.gov/, accessed on 21 January 2022) [14]. Future climate scenarios were projected using four Shared Socioeconomic Pathways (SSPs) and the BCC-CSM2-MR model from the Beijing Climate Center, confirmed as highly effective for simulating climate variations in China [15]. All environmental data were processed at a spatial resolution of 2.5 arc-minutes, covering a rectangular area broadly representing China (18.16°–53.53° N, 73.45°–134.98° E).

We performed a correlation analysis of environmental variables using ENMTools [16]. When the absolute value of the correlation coefficient between two variables surpassed 0.7, we excluded the less influential variable, as indicated by Jackknife test results [17,18].

2.3. Model Optimization and Evaluation Metrics

We employed the ENMeval 2.03 package [19] for model parameter optimization, utilizing 10-fold cross-validation to ensure the stability of the prediction accuracy [20]. We combined eight regularization multipliers, ranging from 0.5 to 4 in 0.5 increments, with six feature classes (linear (L), quadratic (Q), hinge (H), linear–quadratic–hinge (LQH), linear–quadratic–hinge–product (LQHP), and linear–quadratic–hinge–product–threshold (LQHPT)), resulting in a suite of 48 candidate models (8 RM $\times$ 6 FC). The Akaike Information Criterion corrected for small sample sizes (AICc) was employed to compare the goodness of fit and complexity across the models, with models achieving the lowest AICc (Delta AICc = 0) generally indicating superior performance [19].

We also evaluated the model performance using the following metrics: area under the receiver operating characteristic curve (AUC), the Continuous Boyce Index (CBI), the 10% training omission rate (OR10), and the difference between the training and testing AUC (AUCdiff). The AUC, a threshold-independent metric, is commonly utilized to assess the performance of MaxEnt models. Typically, a value of $1 > \text{AUC} \geq 0.9$ indicates excellent predictive performance, while $0.9 > \text{AUC} \geq 0.8$ denotes good performance [21]. The range of the CBI lies between -1 and 1, with values closer to 1 indicating higher consistency between model predictions and the observed distribution in the evaluation dataset [22]. The OR10 is used to demonstrate the degree of model overfitting, with values closer to 0.1 suggesting lower overfitting levels [19]. Similarly, AUCdiff is employed to assess the degree of model overfitting, where its magnitude is directly proportional to the level of overfitting [23].

The final predictions for the suitable habitat distribution of *O. glabra* were conducted using MaxEnt 3.4.4 [24], with the optimal combination of Feature Classes (FC) and Regularization Multipliers (RM) settings, consistent with previous studies [25,26].

2.4. Habitat Suitability Classification and Visualization of Future Changes

The maximum training sensitivity plus specificity logistic (MTSPS) threshold was employed to categorize species habitats into "suitable" and "unsuitable" zones. This methodology has previously been proven to be straightforward and effective [27]. Based on logistic values derived from the model, the habitat of *O. glabra* was segmented into

unsuitable areas (0 to MTSPS), low-suitability areas (MTSPS to 0.4), medium-suitability areas (0.4 to 0.6), and high-suitability areas (0.6 to 1).

The ArcGIS Toolbox was utilized to assign values of 1, 2, 3, and 4 to unsuitable areas and low-, medium-, and high-suitability areas, respectively. This approach facilitates the comparison of current and future distribution patterns of suitable habitats by observing changes in raster values [21]. For instance, a change in raster value from 2 to 4, denoted as "2–4", indicates a transition from a low- to a high-suitability area. Additionally, using SDM-Tools 2.5 [28], the centroids of total suitable areas at different time points were calculated and connected in chronological order to observe the direction of centroid migration.

3. Results

3.1. Occurrence Records and Environmental Variable Screening

A total of 537 occurrence points of *O. glabra* were obtained through field surveys and online databases. After spatial filtering at a 20 km distance, 178 occurrence points remained (see Table S1 for details). Spatial autocorrelation analysis revealed that the distribution of unfiltered occurrence points was clustered, with a Moran's Index of 0.04770; however, after spatial filtering at 20 km, the distribution appeared random, as indicated by the Moran's Index of −0.00056 (Figure 2A). Consequently, we modeled using the spatially filtered occurrence points.

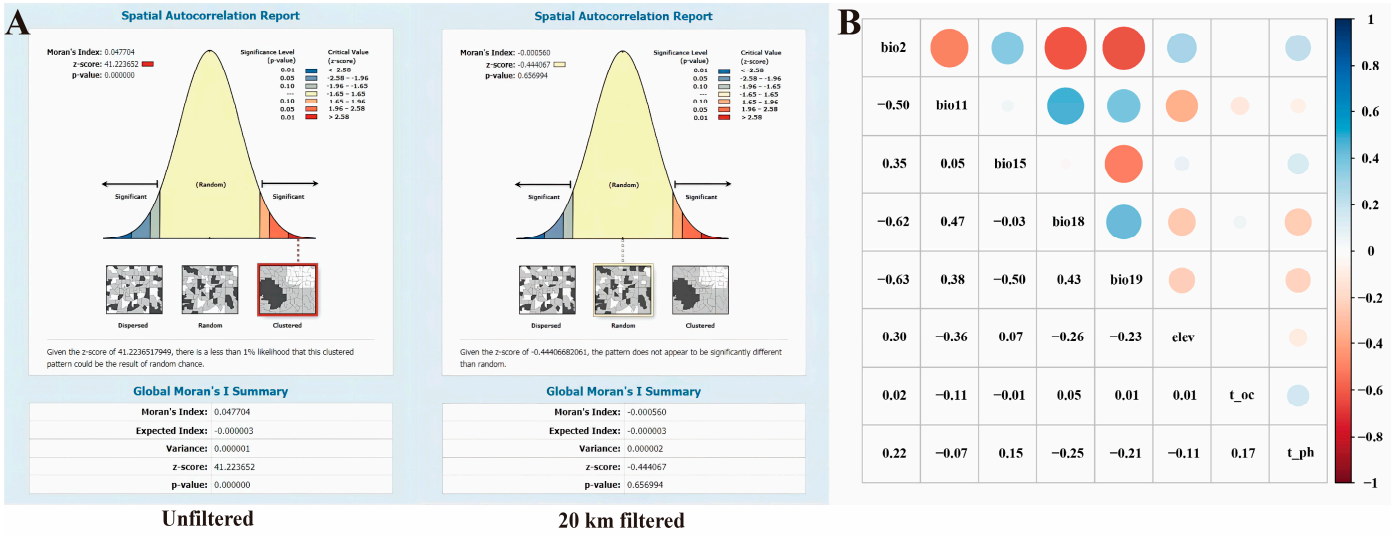

Figure 2. The spatial autocorrelation analysis of occurrences (**A**) and correlations among environmental variables employed in the modeling (**B**).

After filtering 24 environmental variables, the final selection for modeling included the mean diurnal range (bio2), mean temperature of the coldest quarter (bio11), precipitation seasonality (bio15), precipitation of the warmest quarter (bio18), precipitation of the coldest quarter (bio19), elevation (evel), topsoil organic carbon (t_oc), and topsoil pH (t_oh), all with absolute correlation values of less than 0.7 (Figure 2B).

3.2. Model Optimization and Evaluation

Among 48 candidate models, the model configured with the parameters "FC = LQH, RM = 0.5" achieved the lowest AICc value, as shown in Table 1. Compared to the default model, this optimized model exhibited higher AUC and CBI scores and lower OR10 and AUCdiff scores, indicating increased accuracy and diminished overfitting. With an AUC exceeding 0.9, a CBI close to 1, and an OR10 approaching the target of 0.1, this model demonstrates robust predictive performance, making it well-suited for projecting the habitat distribution of *O. glabra*.

Table 1. Comparison of metrics before and after model optimization.

Model	Model Parameter	Avg. AUC	Avg. CBI	Avg. OR10	Avg. AUCdiff	AICc	Delta.AICc
Default	FC = LQPH, RM = 1	0.9461 ± 0.0260	0.8796 ± 0.0681	0.1307 ± 0.1065	0.0222 ± 0.0185	4246.1018	0
Optimized	FC = LQH, RM = 0.5	0.9500 ± 0.0196	0.8832 ± 0.0601	0.1415 ± 0.1018	0.0182 ± 0.0122	4240.9586	5.1431

3.3. Key Environmental Variables

Figure 3A highlights the contribution rates of various environmental variables to the model. The most significant variable was the mean temperature of the coldest quarter, contributing 40.72%. It was followed by precipitation of the coldest quarter, which contributed 22.86%, and precipitation of the warmest quarter, contributing 14.73%. Collectively, these three accounted for 78.31% of the total contributions.

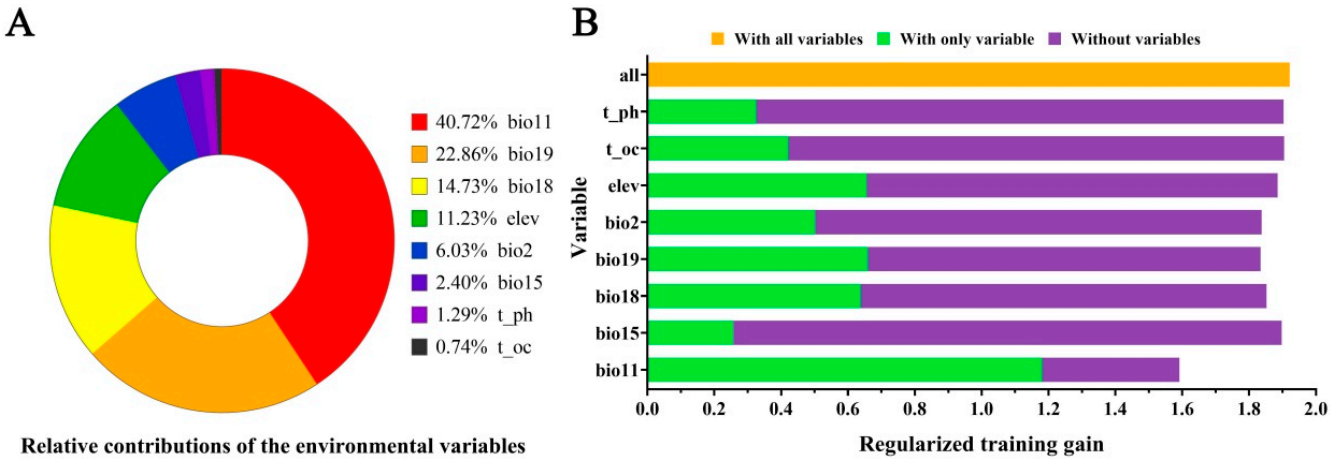

Figure 3. Percentage contribution of the variables (**A**) and results of the jackknife test of variables used for the MaxEnt model (**B**).

The jackknife test, shown in Figure 3B, confirmed the significance of these environmental variables in modeling habitat suitability for *O. glabra*. The largest gain in model accuracy occurred when including the mean temperature of the coldest quarter. This was followed by the contributions from the precipitation of the coldest quarter, elevation, and precipitation of the warmest quarter, indicating that these variables provide critical information for the model.

Excluding the mean temperature of the coldest quarter resulted in the most considerable decrease in model accuracy, followed by the precipitation of the coldest quarter, the mean diurnal range, and the precipitation of the warmest quarter. This pattern shows that these factors offer indispensable information that cannot be substituted by other variables. Therefore, these conditions—specifically the mean temperature of the coldest quarter, precipitation of the coldest quarter, and precipitation of the warmest quarter—play crucial roles in determining the distribution of *O. glabra*.

Figure 4 presents the response curves of environmental variables (with the horizontal axis representing the values of the environmental variables and the vertical axis showing the logistic values from the model) that depict the habitat suitability of *O. glabra* under varying environmental conditions. The response curve for elevation (elev) exhibited two peaks at 1351.26 m and 3187.70 m, with corresponding logistic values of 0.68 and 0.43. The response curve for total potential hydrogen (t_ph) exhibited three peaks at $-\log(H^+)$ values of 5.86, 7.85, and 8.55, corresponding to logistic values of 0.39, 0.72, and 0.96. Apart from elev and t_ph, other environmental variables exhibited approximately unimodal response relationships. Table 2 displays the optimum value of suitability, the highest logistic value, and the suitable habitat threshold for these environmental variables. According to the classification method of "suitable–unsuitable", grid cells with a logistic value exceeding

the minimum threshold for suitable potential species survival (MTSPS) of 0.1872 were categorized as suitable habitats, thereby establishing the suitable habitat threshold for environmental variables.

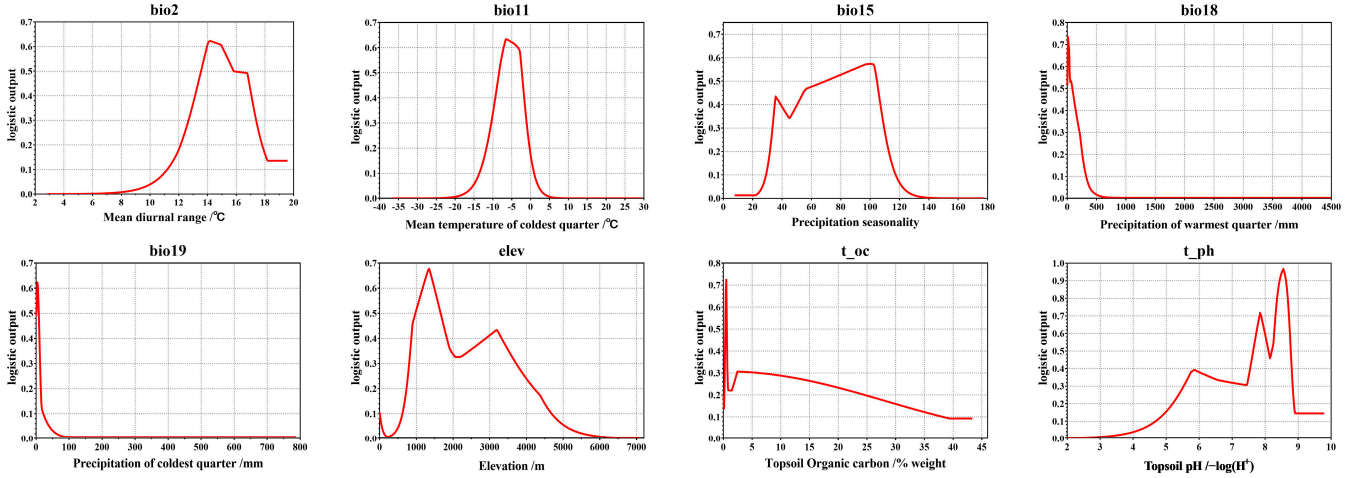

Figure 4. Response curves between logistic outputs and environmental variables utilized in the modeling.

Table 2. Details of environmental variables used for the MaxEnt model.

Environmental Variables	Optimum Value of Suitability	Highest Logistic Value	Suitable Habitat Threshold
bio2	14.22 °C	0.62	11.98~17.91 °C
bio11	−6.49 °C	0.63	−12.04~−0.07 °C
bio15	100.01	0.57	31.22~113.46
bio18	11.44 mm	0.73	0~269.50 mm
bio19	4.01 mm	0.62	0~15.17 mm
elev	1351.26 m	0.68	715.00~4341.35 m
t_oc	0.50% weight	0.72	0~27.45% weight
t_ph	8.55 $-\log(H^+)$	0.96	5.11~8.88 $-\log(H^+)$

3.4. Current Suitable Habitat Distribution

The distribution model for the suitable habitats of *O. glabra* under the current climatic conditions is depicted in Figure 5. The areas classified as low, medium, and high suitability encompass 1.22 × 106 km^2, 5.46 × 105 km^2, and 3.18 × 105 km^2, respectively. The medium- and high-suitability areas are primarily located in the central and western parts of Xinjiang (northern and western Tarim Basin, surrounding areas of Turpan Basin), western and southwestern Inner Mongolia (eastern and western sides of the Badain Jaran Desert, the Tengger Desert and its southern regions, and the Yellow River basin in Inner Mongolia and its southern areas), central and northern Ningxia (Ningxia Yellow River basin area), north–central Gansu (north of the Qilian Mountains), central Qinghai (Altai Mountains area), northern Shaanxi, and central and northern Shanxi. Low-suitability areas are mainly found around the medium- and high-suitability regions, with scattered distributions in northwestern Sichuan, central and southeastern Tibet, and northern Hebei. In addition, we also generated a figure depicting the relationship between the suitability of *O. glabra* and its occurrence records. For further details, please refer to Figure S1.

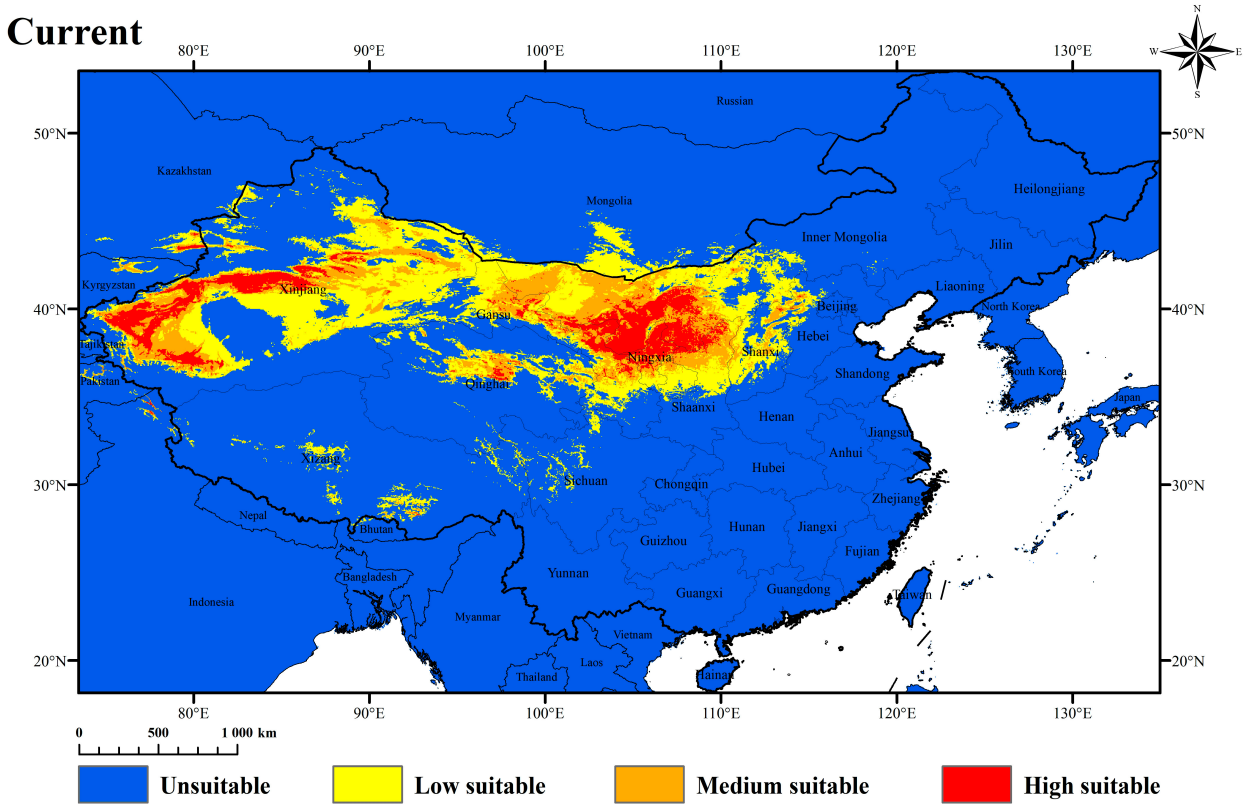

Figure 5. Simulation of suitable habitat distribution of *O. glabra* in current climate conditions.

3.5. Changes in the Distribution of Future Suitable Habitat

Projections of the habitat suitability for *O. glabra* in the 2050s and 2070s were made under four future climate scenarios (Figure S2) and compared with the current spatial distribution of *O. glabra* habitats (Figure 6). Overall, regions where habitat suitability is predicted to decrease are primarily concentrated in the southeastern part of the total habitat area, while increases in suitability are expected mainly in the northern, northwestern, and northeastern sections. Figure 7 illustrates that under all four climate scenarios, the centroid of *O. glabra*'s total habitat area generally shifts towards inland and higher-latitude regions.

We quantified the relative area of each suitability class within the study region under various future climate scenarios, as well as the average elevation of the total suitable habitat area (Table 3). Under all future scenarios, the area of suitable habitats for *O. glabra* is projected to increase relative to the present. In the SSP126 and SSP245 scenarios, the total area of suitable habitat initially increases and subsequently experiences a slight decline; in contrast, under the SSP370 and SSP585 scenarios, it continues to expand. Across all four climate scenarios, the average elevation of the total suitable habitat area consistently increases.

Table 3. Changes in the relative proportions and average elevation of suitable habitat of *O. glabra*.

Period/Climate Scenarios	Current	2050s				2070s			
		SSP126	SSP245	SSP370	SSP585	SSP126	SSP245	SSP370	SSP585
Unsuitable area	87.76%	84.26%	83.04%	84.18%	84.15%	85.46%	83.28%	80.68%	82.08%
Low-suitability area	7.18%	8.83%	8.79%	8.11%	8.15%	7.79%	8.50%	9.55%	9.10%
Medium-suitability area	3.21%	4.35%	4.78%	4.61%	4.27%	4.09%	4.74%	5.57%	4.87%
High-suitability area	1.85%	2.56%	3.39%	3.09%	3.43%	2.66%	3.48%	4.20%	3.95%
All suitable area	12.24%	15.74%	16.96%	15.82%	15.85%	14.54%	16.72%	19.32%	17.92%
Elevation/m	1541.81	1603.58	1677.62	1707.62	1659.24	1634.88	1683.77	1741.18	1762.69

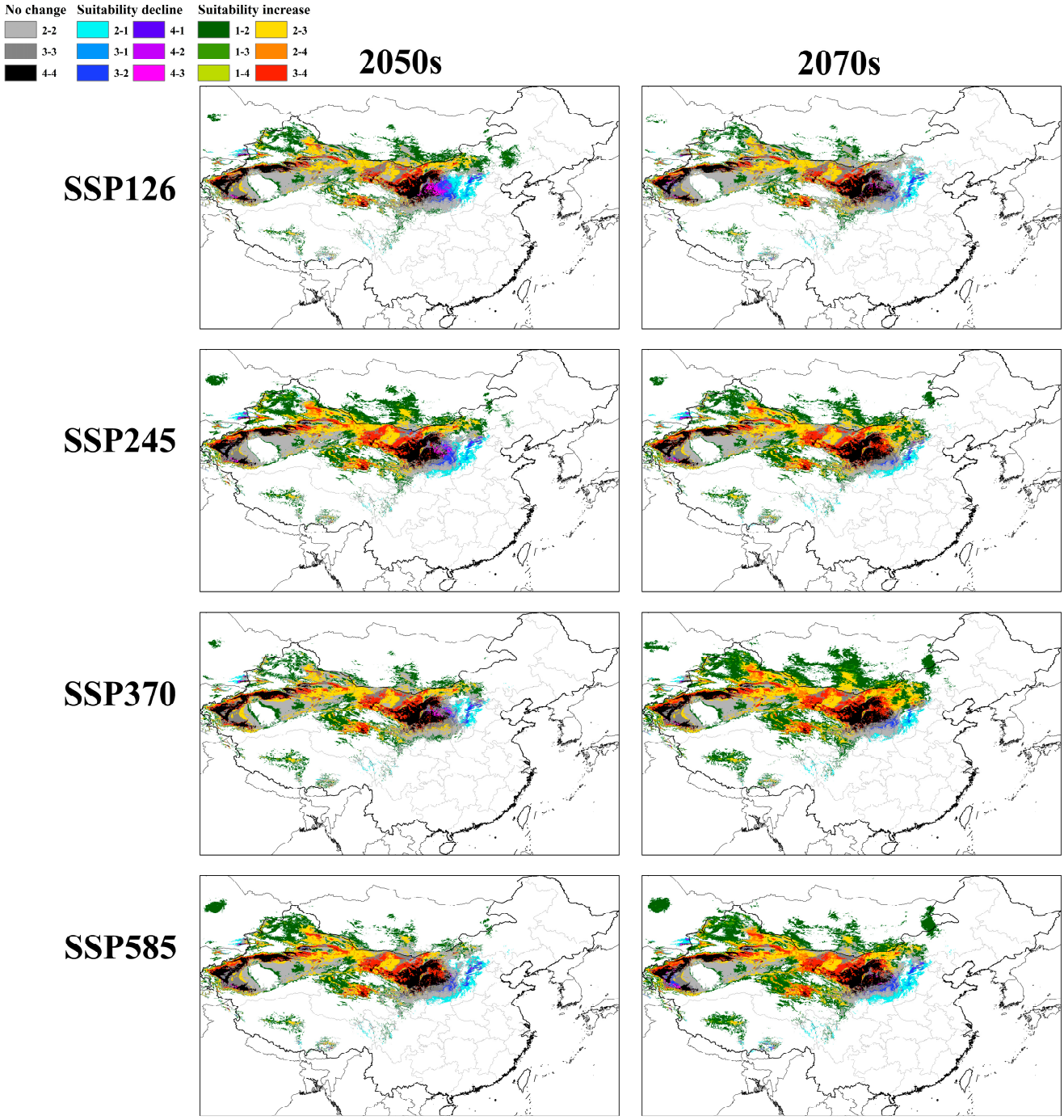

Figure 6. Changes in the area of suitable habitat of *O. glabra* under different future climate conditions relative to those under current climate conditions. "1" indicates unsuitability, "2" indicates low suitability, "3" indicates medium suitability, and "4" indicates high suitability.

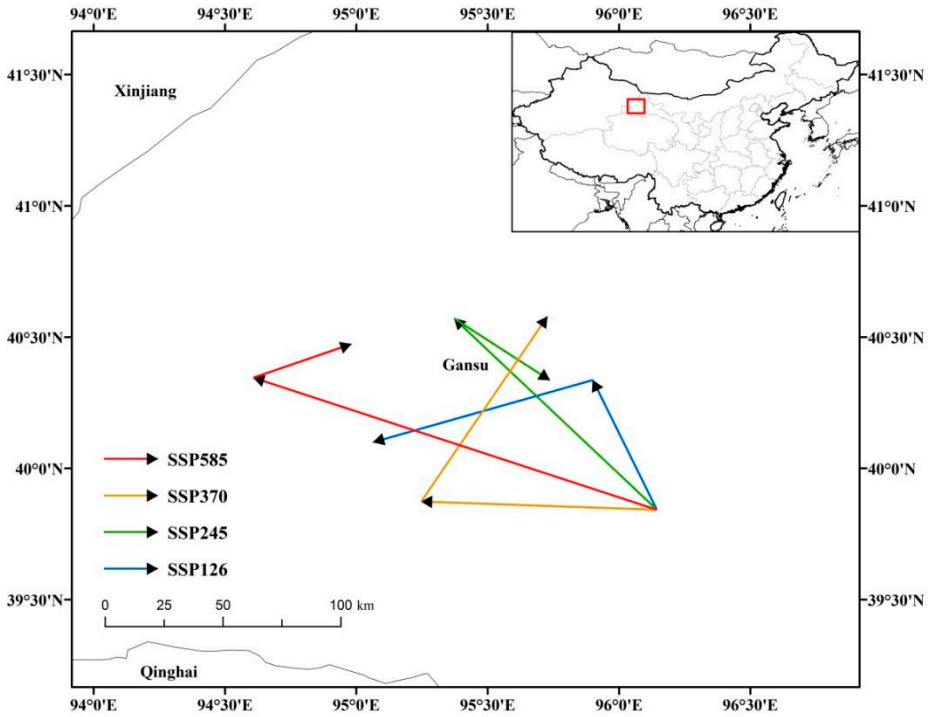

Figure 7. Migration of the centroid of suitable habitat of *O. glabra*.

4. Discussion

4.1. Optimization of MaxEnt Model

The processing of species occurrence data and environmental variables, along with the configuration of MaxEnt model parameters, significantly affects the model's performance. A fundamental assumption of the MaxEnt model is that species occurrence data are either systematically or randomly sampled across all regions [8]. However, in practical surveys, various factors often introduce sampling bias, leading to model overfitting and reduced predictive capacity [29]. To mitigate this, we implemented spatial filtering to reduce the spatial autocorrelation among occurrence points, thereby approximating the random sampling approach. Additionally, multicollinearity among some environmental variables can cause overfitting [30]. We used the ENMTools to assess correlations among these variables and selectively filtered them. Lastly, research indicates that the settings for the feature class (FC) and regularization multiplier (RM) substantially influence the robustness of MaxEnt predictions, with default parameters frequently being suboptimal [31]. Consequently, we employed the ENMeval package to optimize these model parameters. The optimized Maxent model demonstrated an AUC > 0.9, a CBI close to 1, and an OR10 near the desired value of 0.1, confirming the reliability of the model for predicting suitable habitats for *O. glabra*.

4.2. Environmental Variables Affecting the Distribution of O. glabra

Temperature and precipitation are significant factors influencing the geographical distribution of vegetation [32]. Typically, a plant's thermal requirements determine its latitudinal range of suitable habitats, while its moisture needs influence proximity to areas with abundant rainfall, such as coastal versus inland regions [33,34]. This study reveals the key environmental variables and habitat suitability thresholds for *O. glabra*, which are the mean temperature of the coldest quarter (ranging from −12.04 to −0.07 °C), precipitation of the coldest quarter (ranging from 0 to 15.17 mm), and precipitation of the warmest quarter (ranging from 0 to 269.50 mm). Combined with other environmental factors used for modeling, it is evident that *O. glabra* can adapt to cold, dry climates and poor soils, consistent with its known resilience to drought and cold, and vigorous growth characteristics in arid and semi-arid regions [35]. Wang et al. [36] analyzed the soil in several areas within the Alxa Left Banner in Inner Mongolia where *O. glabra* thrives, finding

an average pH of approximately 8. In the study, the soil pH suitability threshold ranged from 5.11 to 8.88, indicating that *O. glabra* can adapt to both mildly alkaline and mildly acidic soils. Moreover, Flora of China noted that *O. glabra* grows at elevations around 2000 m [37]; however, the MaxEnt model suggests a broader range of suitable elevations from 715.00 to 4341.35 m. This discrepancy suggests that some suitable habitats identified by the model may not have been documented previously, indicating a broader elevation range for *O. glabra* than previously recognized.

4.3. Suitable Habitat of O. glabra under Different Climate Conditions

Under the current climatic conditions, the suitable habitats for *O. glabra* are primarily located in provinces such as Xinjiang, Inner Mongolia, Gansu, Qinghai, Ningxia, and Tibet, consistent with previous literature [7]. Additionally, there are potential suitable areas in parts of Sichuan, Shanxi, and Hebei provinces. Under four future climate scenarios, the overall distribution of suitable habitats for *O. glabra* is projected to shift northwestwards and to higher elevations. This shift is likely in response to anticipated increases in temperature and precipitation in northwestern China as the climate warms [38]. Similar trends have been observed in past research; for instance, Lenoir et al. [39] noted that with global warming, the geographical distribution of most European plants is shifting towards higher latitudes and elevations. Beckage et al. [40] reported that the boundary between the broadleaf forests and northern coniferous forests in Vermont, USA, ascended at least 90 m between 1962 and 2005. In China, Wang et al. [41] and Xu et al. [42] predicted a similar northward shift for several common fruit tree species. Notably, under all four future climate scenarios, the total area of suitable habitats for *O. glabra* is expected to increase, with the most significant expansion predicted under the SSP370 scenario for the 2070s, reaching 157.84% of the current suitable area. As depicted in Figure 5, during both future periods under the four climate scenarios, vast regions in central Tibet, central Qinghai, northern Xinjiang, and central Inner Mongolia are likely to become suitable for *O. glabra*, coinciding with areas where grazing is highly prevalent. Given its toxic effects on grazing industries, this finding warrants caution.

4.4. Research Significance and Limitations

The introduction highlights *O. glabra* as a significant toxic weed that adversely affects the grassland livestock industry in China. Its deleterious impacts are threefold: (1) It causes livestock poisoning and death. Swainsonine, a toxic alkaloid in *O. glabra*, inhibits α-mannosidase within animal tissues, leading to vacuolar degeneration and ultimately organ failure and death [6]. (2) It negatively impacts livestock reproduction and impedes breed improvement. Poisoning from *O. glabra* results in infertility, miscarriage, and weak offspring in females, while simultaneously reducing libido and breeding capabilities in males [6]. (3) It impacts the ecological balance of grasslands. With traits like drought resistance, cold tolerance, and strong adversity resistance, *O. glabra* fiercely competes with superior forage for sunlight, soil nutrients, and water [35]. Traditional control measures for such toxic plants include manual removal, herbicides, competitive planting, and biological control, along with preventative measures like medicated feeds, vaccinations, and enhanced pasture management [43]. Additionally, Tao et al. [44] discovered that ensiling *O. glabra* with whole corn in certain proportions reduces its toxic component levels, making it suitable for ruminant feed. Understanding the suitable habitats for toxic plants and how climate change affects their distribution, and visualizing these aspects, are crucial for managing, utilizing, and controlling these plants in pasture management strategies, such as selecting pasture locations, deploying preventive medications and vaccines, and establishing silage feed production bases and control strategies.

Furthermore, the scarcity of *O. glabra* occurrence records in online databases that meet modeling criteria resulted in reduced model accuracy, potentially limiting habitat modeling studies. In this study, we obtained substantial *O. glabra* distribution data through

field surveys and employed optimization techniques to develop a robust model, thereby addressing gaps in previous research.

However, this study also presents certain limitations. While the MaxEnt model exhibits high accuracy, this does not imply that the modeled habitats align perfectly with the actual species distribution [45]. Beyond climatic, topographic, and soil factors, other elements such as interspecies interactions, adaptive capabilities of the species, and grazing activities also impact the distribution of toxic weeds. With current technology, it is challenging to quantify or statistically analyze these factors for model integration. Additionally, predictions about future events are inherently subject to a degree of uncertainty, typically related to the temporal distance of the forecast. These limitations should be considered when referencing and utilizing the model. Nevertheless, species distribution models (SDMs) remain vital tools for predicting suitable habitats under the backdrop of climate change [46].

5. Conclusions

In summary, the optimized MaxEnt model robustly simulates and predicts the distribution of suitable habitats for *O. glabra*. The mean temperature of the coldest quarter (bio11), precipitation of the coldest quarter (bio19), and precipitation of the warmest quarter (bio18) are the critical environmental variables influencing the distribution of *O. glabra*. Currently, *O. glabra* is predominantly found in provinces such as Xinjiang, Inner Mongolia, Gansu, Qinghai, Ningxia, and Tibet. Projections indicate that under four future climate scenarios, the area of suitable habitats for *O. glabra* will increase and shift towards higher latitudes and elevations. This study provides essential data and a theoretical basis for the prevention and control of *O. glabra* and grassland grazing management.

Supplementary Materials: The following supporting information can be downloaded at: https://www.mdpi.com/article/10.3390/agriculture14060850/s1, Table S1: Occurrence data; Table S2: Environmental variables and their type and description; Figure S1: Degree of suitability and occurrence records for *O. glabra*. Figure S2: Projections of the habitat suitability for O. glabra in the 2050s and 2070s.

Author Contributions: Conceptualization, R.H. and B.Z.; methodology, R.H. and B.Z.; software, R.H.; formal analysis, R.H.; investigation, R.H., C.W., X.W. and B.Z.; writing—original draft preparation, R.H.; writing—review and editing, R.H., C.W., H.L. and B.Z.; funding acquisition, B.Z. All authors have read and agreed to the published version of the manuscript.

Funding: This work was supported by the grants from the National Natural Science Foundation (No. 32072928).

Institutional Review Board Statement: Not applicable.

Data Availability Statement: All data are contained within the article or Supplementary Materials.

Conflicts of Interest: The authors declare no conflicts of interest.

References

1. O'Connor, B.; Bojinski, S.; Roosli, C.; Schaepman, M.E. Monitoring global changes in biodiversity and climate essential as ecological crisis intensifies. *Ecol. Inf.* **2020**, *55*, 101033. [CrossRef]
2. Qin, G.-X.; Wu, J.; Li, C.-B.; Qin, A.-N.; Ni, L.; Yao, X.-Q. Grassland vegetation phenology change and its response to climate changes in North China. *J. Appl. Ecol.* **2019**, *30*, 4099–4107. [CrossRef]
3. Stocker, T.F. Climate change. The closing door of climate targets. *Science* **2013**, *339*, 280–282. [CrossRef]
4. Ghahramani, A.; Howden, S.M.; del Prado, A.; Thomas, D.T.; Moore, A.D.; Ji, B.; Ates, S. Climate change impact, adaptation, and mitigation in temperate grazing systems: A review. *Sustainability* **2019**, *11*, 7224. [CrossRef]
5. Zhou, Q.W.; Zhao, B.Y.; Lu, H.; Wang, S.S.; Zhang, L.; Wen, W.L.; Yang, X.W. The Research and Control Situation of Ecology and Animal Poisoning of Locoweed in Western Natural Grassland of China. *Sci. Agric. Sin.* **2013**, *46*, 1280–1296. [CrossRef]
6. Wu, C.C.; Han, T.S.; Lu, H.; Zhao, B.Y. The toxicology mechanism of endophytic fungus and swainsonine in locoweed. *Environ. Toxicol. Pharm.* **2016**, *47*, 38–46. [CrossRef] [PubMed]
7. Guo, R.; Guo, Y.; Wang, S.; Yang, C.; Su, Y.; Wu, C. Adcances in research on poisonous plants and grazing livestock poisoning diseases of Natural Grassland in China. *Acta Vet. Zootech. Sin.* **2021**, *52*, 1171–1185. [CrossRef]

8. Phillips, S.J.; Anderson, R.P.; Schapire, R.E. Maximum entropy modeling of species geographic distributions. *Ecol. Model.* **2006**, *190*, 231–259. [CrossRef]
9. Fois, M.; Cuena-Lombrana, A.; Fenu, G.; Bacchetta, G. Using species distribution models at local scale to guide the search of poorly known species: Review, methodological issues and future directions. *Ecol. Model.* **2018**, *385*, 124–132. [CrossRef]
10. Aiello-Lammens, M.E.; Boria, R.A.; Radosavljevic, A.; Vilela, B.; Anderson, R.P. spThin: An R package for spatial thinning of species occurrence records for use in ecological niche models. *Ecography* **2015**, *38*, 541–545. [CrossRef]
11. Jiang, R.P.; Zou, M.; Qin, Y.; Tan, G.D.; Huang, S.P.; Quan, H.G.; Zhou, J.Y.; Liao, H. Modeling of the Potential Geographical Distribution of Three *Fritillaria* Species Under Climate Change. *Front. Plant Sci.* **2022**, *12*, 749838. [CrossRef] [PubMed]
12. Riahi, K.; van Vuuren, D.P.; Kriegler, E.; Edmonds, J.; O'Neill, B.C.; Fujimori, S.; Bauer, N.; Calvin, K.; Dellink, R.; Fricko, O.; et al. The Shared Socioeconomic Pathways and their energy, land use, and greenhouse gas emissions implications: An overview. *Glob. Environ. Chang.* **2017**, *42*, 153–168. [CrossRef]
13. Fick, S.E.; Hijmans, R.J. WorldClim 2: New 1-km spatial resolution climate surfaces for global land areas. *Int. J. Climatol.* **2017**, *37*, 4302–4315. [CrossRef]
14. Wieder, W.; Boehnert, J.; Bonan, G.; Langseth, M. *Regridded Harmonized World Soil Database v1. 2*; ORNL DAAC: Oak Ridge, TN, USA, 2014.
15. Shi, X.L.; Chen, X.L.; Dai, Y.W.; Hu, G.Q. Climate Sensitivity and Feedbacks of BCC-CSM to Idealized CO_2 Forcing from CMIP5 to CMIP6. *J. Meteorol. Res.* **2020**, *34*, 865–878. [CrossRef]
16. Li, D.; Li, Z.; Liu, Z.; Yang, Y.; Khoso, A.G.; Wang, L.; Liu, D. Climate change simulations revealed potentially drastic shifts in insect community structure and crop yields in China's farmland. *J. Pest. Sci.* **2022**, *96*, 55–69. [CrossRef]
17. Dormann, C.F.; Elith, J.; Bacher, S.; Buchmann, C.; Carl, G.; Carre, G.; Marquez, J.R.G.; Gruber, B.; Lafourcade, B.; Leitao, P.J.; et al. Collinearity: A review of methods to deal with it and a simulation study evaluating their performance. *Ecography* **2013**, *36*, 27–46. [CrossRef]
18. Zeng, Y.W.; Wei, L.B.; Yeo, D.C.J. Novel methods to select environmental variables in MaxEnt: A case study using invasive crayfish. *Ecol. Model.* **2016**, *341*, 5–13. [CrossRef]
19. Muscarella, R.; Galante, P.J.; Soley-Guardia, M.; Boria, R.A.; Kass, J.M.; Uriarte, M.; Anderson, R.P. ENMeval: An R package for conducting spatially independent evaluations and estimating optimal model complexity for MAXENT ecological niche models. *Methods Ecol. Evol.* **2014**, *5*, 1198–1205. [CrossRef]
20. Hundessa, S.; Li, S.S.; Liu, D.; Guo, J.P.; Guo, Y.M.; Zhang, W.Y.; Williams, G. Projecting environmental suitable areas for malaria transmission in China under climate change scenarios. *Environ. Res.* **2018**, *162*, 203–210. [CrossRef]
21. Zhao, Y.C.; Zhao, M.Y.; Zhang, L.; Wang, C.Y.; Xu, Y.L. Predicting Possible Distribution of Tea (*Camellia sinensis* L.) under Climate Change Scenarios Using MaxEnt Model in China. *Agriculture* **2021**, *11*, 1122. [CrossRef]
22. Hirzel, A.H.; Le Lay, G.; Helfer, V.; Randin, C.; Guisan, A. Evaluating the ability of habitat suitability models to predict species presences. *Ecol. Model.* **2006**, *199*, 142–152. [CrossRef]
23. Warren, D.L.; Seifert, S.N. Ecological niche modeling in Maxent: The importance of model complexity and the performance of model selection criteria. *Ecol. Appl.* **2011**, *21*, 335–342. [CrossRef] [PubMed]
24. Phillips, S.J.; Dudik, M. Modeling of species distributions with Maxent: New extensions and a comprehensive evaluation. *Ecography* **2008**, *31*, 161–175. [CrossRef]
25. Huang, R.; Du, H.; Wen, Y.; Zhang, C.; Zhang, M.; Lu, H.; Wu, C.; Zhao, B. Predicting the distribution of suitable habitat of the poisonous weed *Astragalus variabilis* in China under current and future climate conditions. *Front. Plant Sci.* **2022**, *13*, 921310. [CrossRef] [PubMed]
26. Xu, W.; Du, Q.; Yan, S.; Cao, Y.; Liu, X.; Guan, D.X.; Ma, L.Q. Geographical distribution of As-hyperaccumulator Pteris vittata in China: Environmental factors and climate changes. *Sci. Total Environ.* **2021**, *803*, 149864. [CrossRef] [PubMed]
27. Kong, W.Y.; Li, X.H.; Zou, H.F. Optimizing MaxEnt model in the prediction of species distribution. *Chin. J. Appl. Ecol.* **2019**, *30*, 2116–2128. [CrossRef] [PubMed]
28. Brown, J.L.; Bennett, J.R.; French, C.M. SDMtoolbox 2.0: The next generation Python-based GIS toolkit for landscape genetic, biogeographic and species distribution model analyses. *Peerj* **2017**, *5*, e4095. [CrossRef] [PubMed]
29. Warren, D.L.; Wright, A.N.; Seifert, S.N.; Shaffer, H.B. Incorporating model complexity and spatial sampling bias into ecological niche models of climate change risks faced by 90 California vertebrate species of concern. *Divers. Distrib.* **2014**, *20*, 334–343. [CrossRef]
30. Sillero, N. What does ecological modelling model? A proposed classification of ecological niche models based on their underlying methods. *Ecol. Model.* **2011**, *222*, 1343–1346. [CrossRef]
31. Yan, H.Y.; Feng, L.; Zhao, Y.F.; Feng, L.; Wu, D.; Zhu, C.P. Prediction of the spatial distribution of *Alternanthera philoxeroides* in China based on ArcGIS and MaxEnt. *Glob. Ecol. Conserv.* **2020**, *21*, e00856. [CrossRef]
32. Yang, Y.; Li, X.; Kong, X.; Ma, L.; Hu, X.; Yang, Y. Transcriptome analysis reveals diversified adaptation of *Stipa purpurea* along a drought gradient on the Tibetan Plateau. *Funct. Integr. Genom.* **2015**, *15*, 295–307. [CrossRef] [PubMed]
33. Noor, M.; Rehman, N.u.; Jalil, A.; Fahad, S.; Adnan, M.; Wahid, F.; Saud, S.; Hassan, S. Climate change and costal plant lives. In *Environment, Climate, Plant and Vegetation Growth*; Springer: Cham, Switzerland, 2020; pp. 93–108. [CrossRef]

34. Hessburg, P.F.; Miller, C.L.; Parks, S.A.; Povak, N.A.; Taylor, A.H.; Higuera, P.E.; Prichard, S.J.; North, M.P.; Collins, B.M.; Hurteau, M.D. Climate, environment, and disturbance history govern resilience of western North American forests. *Front. Ecol. Evol.* **2019**, *7*, 239. [CrossRef]
35. Wang, S.; Zhang, L.; Chen, G.; Xi, L.; Ma, C. An Overview of Ecological Research on *Oxytropis glabra* DC. *J. Domest. Anim. Ecol.* **2014**, *35*, 85–88.
36. Wang, Q.; Pang, Z.; Li, C.; Wu, J.; Da, N.; Wang, D.; Ma, Q. Effects of *Astragalus variabilis* and *Oxytropis glabra* on the Soil Properties of Desert Grassland. *Acta Agrestia Sin.* **2015**, *23*, 469–475. [CrossRef]
37. Editorial Committee of Chinese Flora, CAOS. *Flora of China Vol.42 Division 1 Leguminosae*; Science Press: Beijing, China, 1998; Volume 42.
38. Wang, C.H.; Zhang, S.N.; Zhang, F.M.; Li, K.C.; Yang, K. On the Increase of Precipitation in the Northwestern China Under the Global Warming. *Adv. Earth Sci.* **2021**, *36*, 980–989. [CrossRef]
39. Lenoir, J.; Gegout, J.C.; Marquet, P.A.; de Ruffray, P.; Brisse, H. A significant upward shift in plant species optimum elevation during the 20th century. *Science* **2008**, *320*, 1768–1771. [CrossRef] [PubMed]
40. Beckage, B.; Osborne, B.; Gavin, D.G.; Pucko, C.; Siccama, T.; Perkins, T. A rapid upward shift of a forest ecotone during 40 years of warming in the Green Mountains of Vermont. *Proc. Natl. Acad. Sci. USA* **2008**, *105*, 4197–4202. [CrossRef] [PubMed]
41. Wang, M.; Hu, Z.; Wang, Y.; Zhao, W. Spatial Distribution Characteristics of Suitable Planting Areas for *Pyrus* Species under Climate Change in China. *Plants* **2023**, *12*, 1559. [CrossRef] [PubMed]
42. Xu, W.; Miao, Y.; Zhu, S.; Cheng, J.; Jin, J. Modelling the Geographical Distribution Pattern of Apple Trees on the Loess Plateau, China. *Agriculture* **2023**, *13*, 291. [CrossRef]
43. FU JJ, G.; HUANG, W. The distribution of locoweed in natural grassland in the United States and the current status and prospects of research on animal poisoning. *Acta Agrestia Sin.* **2019**, *27*, 519–530. [CrossRef]
44. Tao, Y.; Niu, D.; Li, F.; Zuo, S.; Sun, Q.; Xu, C. Effects of Ensiling *Oxytropis glabra* with Whole-Plant Corn at Different Proportions on Fermentation Quality, Alkaloid Swainsonine Content, and Lactic Acid Bacteria Populations. *Animals* **2020**, *10*, 1733. [CrossRef] [PubMed]
45. Gebrewahid, Y.; Abrehe, S.; Meresa, E.; Eyasu, G.; Abay, K.; Gebreab, G.; Kidanemariam, K.; Adissu, G.; Abreha, G.; Darcha, G. Current and future predicting potential areas of *Oxytenanthera abyssinica* (*A. Richard*) using MaxEnt model under climate change in Northern Ethiopia. *Ecol. Process* **2020**, *9*, 6. [CrossRef]
46. Wiens, J.A.; Stralberg, D.; Jongsomjit, D.; Howell, C.A.; Snyder, M.A. Niches, models, and climate change: Assessing the assumptions and uncertainties. *Proc. Natl. Acad. Sci. USA* **2009**, *106*, 19729–19736. [CrossRef] [PubMed]